ISBN: 978-3-95450-214-1 ISSN: 2673-5490 doi:10.18429/JACoW-IPAC2021-THPAB009

A HARD X-RAY COMPTON SOURCE AT CBETA

K. Deitrick*, G. H. Hoffstaetter, CLASSE, Cornell University, Ithaca, New York, USA
C. Franck, LASSP, Cornell University, Ithaca, New York, USA
B. D. Muratori, H. Owen, P. H. Williams,
STFC Daresbury Laboratory & Cockcroft Institute, Warrington, UK
G. A. Krafft[1], B. Terzić
Center for Accelerator Science, Old Dominion University, Norfolk, Virginia, USA
J. Crone, University of Manchester & Cockcroft Institute, Manchester, UK
[1]also at Thomas Jefferson National Accelerator Facility, Newport News, Virginia, USA

Abstract

Inverse Compton scattering (ICS) holds the potential for future high flux, narrow bandwidth x-ray sources driven by high quality, high repetition rate electron beams. CBETA, the Cornell-BNL Energy recovery linac (ERL) Test Accelerator, is the world's first superconducting radiofrequency multi-turn ERL, with a maximum energy of 150 MeV, capable of ICS production of x-rays above 400 keV. We present an update on the bypass design and anticipated parameters of a compact ICS source at CBETA. X-ray parameters from the CBETA ICS are compared to those of leading synchrotron radiation facilities, demonstrating that, above a few hundred keV, photon beams produced by ICS outperform those produced by undulators in term of flux and brilliance.

INVERSE COMPTON SCATTERING

Inverse Compton scattering is the process of scattering a photon from a relativistic electron; the energy of the scattered photons from this interaction, taking electron recoil into account, is given by $E_\gamma = E_{\text{laser}}(1-\beta\cos\phi')/\left(1-\beta\cos\theta+(1-\cos\theta')E_{\text{laser}}/E_e\right)$, where $E_e=\gamma m_e c^2$ is the incident total electron energy, γ is the Lorentz factor, m_e is the mass of the electron, c is the speed of light, E_{laser} is the incident photon energy, β is the average speed of the electrons as a fraction of the speed of light, θ is the angle between the incident electrons and the outgoing scattered photons, and ϕ' is the angle between the incident electrons and incident photons. $\theta'=\phi'-\theta$ is the angle between the incident and scattered photons and $\phi=\pi-\phi'$ is the crossing angle [1, 2].

The highest energy photons are backscattered ($\theta=0$) in a head-on collision ($\phi'=\pi$); this maximum energy is referred to as the Compton edge and is given by $E_\gamma^{\max} = 4\gamma^2 E_{\text{laser}}/(1+X)$ where $X=4\gamma E_{\text{laser}}/m_e c^2$ is the electron recoil parameter [3]. For the Thomson regime, collisions occur where the electron recoil is negligible ($X \ll 1$).

For a collision between a bunch of N_e electrons and a laser pulse of N_{laser} photons, the total number of scattered photons N_γ for crossing angle ϕ is given by

$$N_\gamma = \sigma_c \frac{N_e N_{\text{laser}} \cos(\phi/2)}{2\pi\sigma_y\sqrt{\sigma_x^2\cos^2(\phi/2)+\sigma_z^2\sin^2(\phi/2)}}, \quad (1)$$

where σ_c is the Compton scattering cross-section and $\sigma_i^2 = \sigma_{\text{electron},i}^2 + \sigma_{\text{laser},i}^2$ is the convoluted spot size of the electron and laser beam in each direction ($i=x,y,z$) at the interaction point (IP) [4]. In the Thomson regime, $\sigma_c \simeq \sigma_T(1-X)$, where σ_T is the Thomson cross section of 6.65×10^{-29} m^2 [5]. Assuming the incident laser can be approximated as a plane wave, the number of scattered photons within a 0.1% bandwidth at the Compton edge is $N_{0.1\%} \simeq 1.5\times10^{-3}N_\gamma$. Consequently, the rate of photons (flux) into this bandwidth is given by $\mathscr{F}_{0.1\%} \simeq 1.5\times10^{-3}\dot{N_\gamma}$, where $\mathscr{F}=fN_\gamma$ is the total uncollimated flux and f is the repetition rate. In the nondiffraction-limited case for a round beam, where the laser spot at the IP is significantly larger than the electron spot size, the average brilliance is $\mathscr{B}_{\text{avg}} \simeq \frac{\gamma^2\mathscr{F}_{0.1\%}}{4\pi^2\epsilon_N^2}$, where ϵ_N is the normalized transverse emittance of the electron beam at the IP [1, 6].

The bandwidth of the scattered radiation has contributions from the energy spread of the incident electron and laser beams, emittance of the electron beam, and collimation. Typically, the collimation and emittance terms are dominant, so the scattered radiation rms bandwidth $\Delta E_\gamma/E_\gamma$ has the relationship from [3]

$$\frac{\Delta E_\gamma}{E_\gamma} > \sqrt{\left(\frac{1}{\sqrt{12}}\frac{\Psi^2}{1+X+\Psi^2/2}\right)^2+\left(\frac{2\gamma\epsilon_N}{(1+X)\beta^*}\right)^2}, \quad (2)$$

where $\Psi=\gamma\theta_{\text{col}}$ is called the acceptance angle, θ_{col} is the collimation angle, and β^* is the β-function at the IP. This results in a set of combinations of β^* and θ_{col} that will satisfy a particular bandwidth. Each of these solutions will yield a different collimated flux; obviously the desire is to maximize this value. The collimated flux $\mathscr{F}_\Psi$ can be calculated for small collimation angles ($\gamma\theta_{\text{col}}<1$) with $\mathscr{F}_\Psi \propto \left(1+\sqrt[3]{X}\Psi^2/3\right)\Psi^2/\left\{\left[1+(1+X/2)\,\Psi^2\right]\left(1+\Psi^2\right)\right\}$ [7]; for a more detailed explanation of the process of optimizing β^* and θ_{col}, please refer to [8].

ICS AT CBETA

CBETA, the Cornell-BNL (Brookhaven National Lab) ERL Test Accelerator, is an SRF multi-turn ERL using Non-Scaling Fixed Field Alternating-gradient (NS-FFA) arcs, depicted by the gray beamline elements in Fig. 1 [9–11]. The FFA arc consists of permanent Halbach magnets and has an

* kd324@cornell.edu

ISBN: 978-3-95450-214-1 ISSN: 2673-5490 doi:10.18429/JACoW-IPAC2021-THPAB009

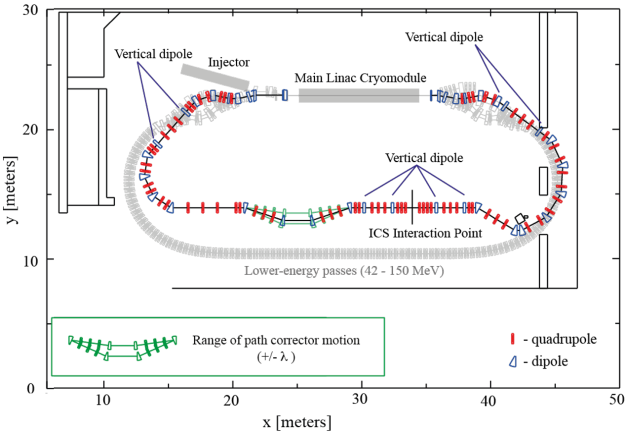

Figure 1: Layout of the ICS bypass in CBETA; grayed beamline elements are already installed in the existing accelerator.

energy acceptance from 42 to 150 MeV. The electron beam is injected at 6 MeV, before accelerating up to 150 MeV in 4 passes; the intermediate energies of 42, 78, and 114 MeV occur after the first, second, and third pass, respectively. In the SX and RX sections, each beam energy passes through a different splitter; this allows for individual control of select beam properties.

The baseline electron beam parameters are shown in Table 1; these maximize the uncollimated flux and associated average brilliance. Using the procedure described in the previous section to select parameters for a specific bandwidth, we have also developed electron beam spot sizes and collimation angles optimized for a 0.5% bandwidth, shown in Table 2; all other electron beam properties remain unchanged from Table 1. The interaction laser is based on existing and state-of-the-art systems – the relevant parameters are given in Table 3. Using these values, the anticipated x-ray parameters can be calculated and are shown in Table 4.

For the top electron energy of 150 MeV and spot size for a 0.5% bandwidth, the anticipated spectra, shown in Fig. 2 was calculated for a head-on collision using the ICCS3D [12] and ICARUS codes. ICCS3D calculates the interaction between a 3D laser pulse and an electron beam described by either typical parameters or an arbitrary distribution; in this case, electrons were tracked through the bypass lattice to the IP using TAO [13, 14] and the resulting distribution was used by ICCS3D. ICARUS, the inverse Compton scattering semianalytic recoil-correct ultrarelativistic spectrum code, uses a modified and corrected[1] version of the 2D formalism of [15], assuming a head-on collision of a laser pulse and electron bunch with Gaussian distributions. Both codes agree well with each other and the analytical results from the formula, once the reduction of flux (roughly a factor of 5) due to the non-zero crossing angle is taken into account.

To use CBETA as an ICS source, a bypass line is required to replace the existing fourth pass due to stringent space

[1] Note that there is an error in Equation 53 of Sun's paper, where the prefactor gives that $dN/dE \propto L^2$ for a source-to-collimator distance L. Clearly, this should be $dN/dE \propto 1/L^2$; the other parts of the given equation are correct.

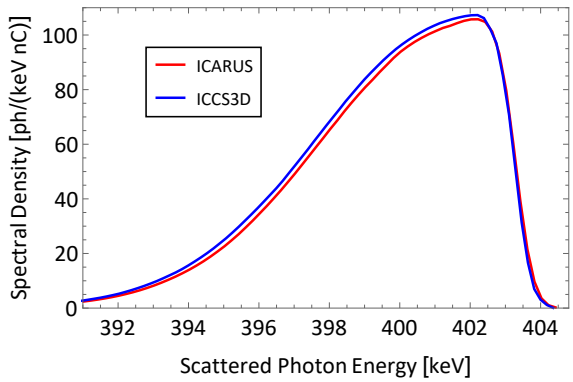

Figure 2: Predicted spectral output (flux) for a head-on collision with the E_e = 150 MeV electrons optimized for a 0.5% bandwidth; this spectrum was generated using the ICCS3D and ICARUS codes for a single bunch-pulse interaction.

Table 1: Baseline Electron Beam Parameters at the CBETA ICS IP; These Values Apply to the Four Electron Energies of 42, 78, 114, and 150 MeV

Parameter	Quantity	Unit
Repetition rate, f	162.5	MHz
Bunch charge, eN_e	32	pC
Transverse normalized *rms* emittance, ϵ_N	0.3	mm-mrad
rms bunch length, $\Delta\tau$	1.0 (3.33)	mm (ps)
Relative energy spread	5.0×10^{-4}	
β at the IP, β^*	1	cm

Table 2: The Optimized Values of the Electron Beam Spot Sizes and Collimation Angles Where We Have Maximized the Flux into a 0.5% Scattered Photon Bandwidth

Parameter	Electron Kinetic Energy (MeV) 42	78	114	150	Unit
β^*	3.56	6.58	9.60	12.62	cm
Electron spot size	11.34	11.34	11.34	11.34	μm
Collimation angle	1.533	0.830	0.569	0.433	mrad

Table 3: Laser Pulse Parameters at the IP

Parameter	Quantity	Unit
Wavelength, λ_{laser}	1064	nm
Photon energy, E_{laser}	1.17	eV
Pulse energy	62	μJ
Number of photons, N_{laser}	3.3×10^{14}	
Repetition rate, f	162.5	MHz
Spot size at the IP, σ_{laser}	25	μm
Crossing angle, ϕ	5	deg
Pulse length	10	ps
Relative energy spread	6.57×10^{-4}	

ISBN: 978-3-95450-214-1 ISSN: 2673-5490 doi:10.18429/JACoW-IPAC2021-THPAB009

Table 4: Anticipated X-ray Parameters, Both Baseline (Top) and Optimized for a 0.5% Bandwidth (Bottom), for the Four Electron Beam Energies of CBETA

Parameter	Electron Kinetic Energy (MeV) 42	78	114	150	Unit
X-ray peak energy	32.2	109.7	233.1	402.5	keV
Source Size	5.84	4.35	3.62	3.17	μm
Uncollimated flux	3.16×10^{10}	3.20×10^{10}	3.21×10^{10}	3.22×10^{10}	ph/s
Spectral density	9.82×10^{5}	2.92×10^{5}	1.38×10^{5}	8.00×10^{4}	ph/s eV
Average brilliance	9.23×10^{10}	3.19×10^{11}	6.81×10^{11}	1.18×10^{12}	ph/s mm^2 mrad^2 0.1% bw
Peak brilliance	2.80×10^{15}	1.00×10^{16}	2.18×10^{16}	3.80×10^{16}	ph/s mm^2 mrad^2 0.1% bw
0.5% bandwidth					
Source Size	10.25	10.34	10.32	10.35	μm
Collimated flux	2.09×10^{8}	2.09×10^{8}	2.09×10^{8}	2.09×10^{8}	ph/s 0.5% bw

restrictions in the existing FFA arc. The layout of the bypass line, designed using BMAD and TAO, is shown by the colored beam line elements in Fig. 1. A system of vertical doglegs, inserted into the energy-specific splitter lines, elevates the bypass above the existing machine; the FFA arc must remain in place to transport the lower energy passes before and after the bypass. Another set of vertical doglegs is present around the IP for extraction of the generated x-rays out of the CBETA machine enclosure; the quadrupoles around the IP provide for the flexible tuning of x-ray bandwidth. The IP is followed by a 4-dipole moving chicane to provide path length adjustment, based on [16]. For a more detailed description of the bypass lattice and its optics, please refer to [8].

COMPARISON TO SYNCHROTRON RADIATION FACILITIES

It is widely acknowledged that the flux and brilliance offered by ICS sources are not competitive at the photon energies typically produced by synchrotron radiation (SR) facilities [1]; many of the ICS sources recently designed are intended to serve as compromises between typical laboratory-scale x-ray sources and large SR facilities in terms of size, cost, access, availability, and x-ray quality [6] and often do not produce x-rays with an energy higher than 200 keV, if that. At x-ray energies above 300 keV, anticipated x-rays produced by ICS sources have a greater flux and average brilliance than those produced at third-generation SR facilities [8]; Fig. 3 compares on-sample measured fluxes from various SR facilities and anticipated fluxes from the CBETA ICS and scaling the CBETA electron beam parameters to 300 MeV (1600 keV photons) and 600 MeV (6360 keV photons). As discussed in [8], multiple 100 keV sources enable vital applications such as thick sample imaging and spectroscopy throughout the periodic chart; at the very highest energies in Fig. 3, ICS sources are in a class by themselves for nuclear material assays through resonance fluorescence.

CONCLUSION

In this paper, we provided a compelling case for the use and feasibility of ERL-driven ICS sources and examined

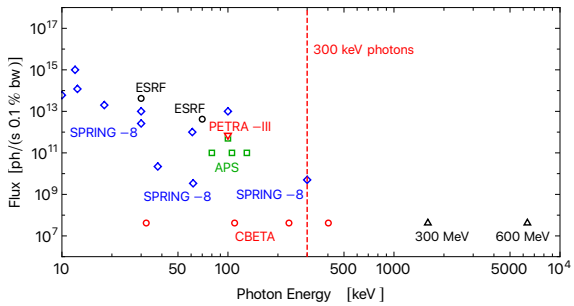

Figure 3: On-sample measured fluxes from APS, ESRF-EBS, PETRA-III, and SPRING-8 for which information has been published [17–20], compared with the predicted CBETA outputs at the 4 discrete photon energies from 32 to 402 keV, and the predicted flux obtained by scaling the CBETA electron energy to 300 MeV (1600 keV photons) and 600 MeV (6360 keV photons).

in detail the performance of an existing multi-turn ERL, CBETA, adapted into such a source, while describing the designed bypass transport line necessary for such an adaptation. We establish that such a source is capable of producing quasimonochromatic photons from the 100s of keV up to the MeV-scale, which is not yet fully served by existing sources. We compared anticipated photon performance of ERL-driven ICS sources to existing large storage-ring-based facilities and demonstrated that in size and performance, the ICS sources proved competitive for photon energies greater than 300 keV.

ACKNOWLEDGEMENTS

This work was supported by NSF Grant No. DMR-0807731, DOE Award No. DE-SC0012704, and by the Science and Technology Facilities Council under Grant Nos. ST/G008248/1 and ST/S505523/1. B.T. was supported by the NSF CAREER Grant No. 1847771. G.K. was supported at Jefferson Lab by U.S. DOE Contract No. DE-AC05-06OR23177. We would like to thank Stanislav Stoupin for useful discussions.

ISBN: 978-3-95450-214-1 ISSN: 2673-5490 doi:10.18429/JACoW-IPAC2021-THPAB009

REFERENCES

[1] G. A. Krafft and G. Priebe, "Compton Sources of Electromagnetic Radiation", *Rev. Accel. Sci. Techol.*, vol. 03, pp. 147-163, 2010. doi:10.1142/S1793626810000440

[2] C. Sun, J. Li, G. Rusev, A. Tonchev, and Y. Wu, "Energy and energy spread measurements of an electron beam by Compton scattering method", *Phys. Rev. ST Accel. Beams*, vol. 12, p. 062801, Jun. 2009. doi:10.1103/PhysRevSTAB.12.062801

[3] N. Ranjan *et al.*, "Simulation of inverse Compton scattering and its implications on the scattered linewidth", *Phys. Rev. Accel. Beams*, vol. 21, p. 030701, Mar. 2018. doi:10.1103/PhysRevAccelBeams.21.030701

[4] T. Suzuki, "General formulae of luminosity for various types of colliding beam machines", High Energy Accelerator Research Organization, Tsukuba, Ibaraki, Japan, Rep. KEK-76-3, 1976.

[5] T. Akagi *et al.*, "Narrow-band photon beam via laser Compton scattering in an energy recovery linac", *Phys. Rev. Accel. Beams*, vol. 19, p. 114701, Nov. 2016. doi:10.1103/PhysRevAccelBeams.19.114701

[6] K. E. Deitrick, G. A. Krafft, B. Terzić, and J. R. Delayen, "High-brilliance, high-flux compact inverse Compton light source", *Phys. Rev. Accel. Beams*, vol. 21, p. 080703, Aug. 2018. doi:10.1103/PhysRevAccelBeams.21.080703

[7] C. Curatolo, I. Drebot, V. Petrillo, and L. Serafini, "Analytical description of photon beam phase spaces in inverse Compton scattering sources", *Phys. Rev. Accel. Beams*, vol. 20, p. 080701, Aug. 2017. doi:10.1103/PhysRevAccelBeams.20.080701

[8] K. Deitrick *et al.*, "Intense monochromatic photons above 100 keV from an inverse Compton source", *Physical Review Accelerators and Beams*, vol. 24, p. 050701, May 2021. doi:10.1103/PhysRevAccelBeams.24.050701

[9] A. Bartnik *et al.*, "CBETA: First Multipass Superconducting Linear Accelerator with Energy Recovery", *Physical Review Letters*, vol. 125, p. 044803, Jul. 2020. doi:10.1103/PhysRevLett.125.044803

[10] G. H. Hoffstaetter *et al.*, "CBETA Design Report, Cornell-BNL ERL Test Accelerator", 2017. arXiv:1706.04245

[11] C. Gulliford *et al.*, "Measurement of the per cavity energy recovery efficiency in the single turn Cornell-Brookhaven ERL Test Accelerator configuration", *Physical Review Accelerators and Beams*, vol. 24, p. 010101, Jan. 2021. doi:10.1103/PhysRevAccelBeams.24.010101

[12] B. Terzić *et al.*, "Improving performance of inverse Compton sources through laser chirping", *Europhys. Lett.*, vol. 126, p. 12003, May 2019. doi:10.1209/0295-5075/126/12003

[13] D. Sagan, The Bmad Manual, https://www.classe.cornell.edu/bmad/manual.html

[14] D. Sagan, The Tao Manual, https://www.classe.cornell.edu/bmad/tao.html

[15] C. Sun and Y. K. Wu, "Theoretical and simulation studies of characteristics of a Compton light source", *Phys. Rev. ST Accel. Beams*, vol. 14, p. 044701, April 2011. doi:10.1103/PhysRevSTAB.14.044701

[16] H. L. Owen and P. H. Williams, "A modular path length corrector for recirculating linacs", *Nucl. Instrum. Methods Phys. Res. Sect. A*, vol. 662, pp. 12-20, 2012.

[17] ESRF-EBS beam line list, https://www.esrf.eu/home/UsersAndScience/Accelerators/ebs---extremely-brilliant-source/ebs-parameters.html

[18] APS beam line list, https://www.aps.anl.gov/Beamlines/Directory

[19] SPRING-8 beam line list, http://www.spring8.or.jp/en/about_us/whats_sp8/facilities/bl/list/.

[20] PETRA III Beam Line List, https://photon-science.desy.de/facilities/petra_iii/beamlines/index_eng.html